Stellar Coronae in Saturated and Supersaturated late-type stars

D.Garcia-Alvarez[1,2], J.J.Drake[2], V.Kashyap[2], L.Lin[2]
[1]Imperial College London, Blackett Lab., Prince Consort Road, London, SW7 2AZ, UK (d.garcia-alvarez@imperial.ac.uk)
[2]Harvard-Smithsonian CfA, 60 Garden St., Cambridge, MA-02138, USA

ABSTRACT

AB Dor, Speedy Mic and Rst 137B are in their early post-T Tauri evolutionary phase (~30-100Myr), at the age of fastest rotation in the life of late-type stars. They straddle the coronal saturation-supersaturation boundary first defined by young stars in open clusters. High resolution *Chandra* X-ray spectra have been analysed to study their coronal properties as a function of coronal activity parameters Rossby number, L_x/L_{bol} and a coronal temperature index. A larger sample comprising our three targets and 22 active stars, observed with *Chandra* and *XMM-Newton* and studied in the recent literature, reveals numerous contrasting features and trends.

ABDOR, SPEEDY MIC AND RST 137B:

Pipeline-processed photon event lists were reduced using CIAO 3.2 and were analysed using the IDL-based PINTofALE software (Kashyap & Drake 2000, BASI, 28, 475). The analysis performed consisted of line identification and fitting, reconstruction of the plasma emission measure distribution including allowance for blending of the diagnostic lines used, and finally, determination of the element abundances.

Summary of Stellar Parameters and Observations.

Star	Sp. Type	B-V	P_{rot}	T_{eff} [K]	$v\sin i$ [km s^{-1}]	log L_x/L_{bol}	ObsID	Instrument	Exp [ks]
AB Dor	K0-2V	0.80	12hr	5250	93	~-3	16	HETG+ACIS-S	52
Speedy Mic	K3V	0.94	9hr	4750	132	<-3	2536/3491	HETG+ACIS-S	35/35
RST137B	M0V	1.60	<9hr	3250	50	~-3	16	HETG+ACIS-S	52

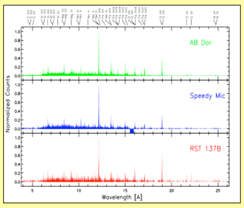

Chandra X-ray HETG-ACIS-S spectra. The strongest lines over the observed wavelength range are identified.

SATURATED-SUPERSATURATED STARS:

In low-mass main sequence (MS) stars, internal structure is determined primarily by stellar mass rather than age. In contrast, surface activity as manifested in X-rays, at least for late-type dwarfs, seems to scale directly with rotation and by consequence with age, but is only slightly dependent on mass (Skumanich 1972, ApJ, 171, 565). Garcia-Alvarez et al. (2005, ApJ, 621, 1009) suggested that the exact evolutionary state of a main-sequence star has little effect on coronal characteristics, and that the parameters that dominate coronal structure and composition are simply the rotation rate and spectral type. Observations suggest that, compared to the Sun, stars of increasing rotation rate show a rise in their X-ray emission that reaches a maximum of about $L_x/L_{\odot}=10^{-3}$ at rotation rates of about P_{rot}=2-4.5d. Beyond this rotation rate is the *saturated* regime where the X-ray luminosity is independent of rotation rate. This behaviour persists until rotation rates of about P_{rot}~0.5d, where the X-ray luminosity begins to decrease again. This regime is referred to as *supersaturated* (Prosser 1996, AJ, 112, 1570; Randich 1998, ASP Conf. Ser., 154, 501). Although a number of different explanations have been invoked in order to explain the *saturation* and *supersaturation* phenomenon (Jardine 2004, A&A, 414, L5; Ryan et al. 2005, 433, 323) there is currently no consensus.

CORONAE OF FAST ROTATORS (SINGLE STARS AND BINARY SYSTEMS)

We compare the derived coronal DEMs and chemical composition for both fast rotators in single stars and binary systems reported in previous works (see Table). In order to compare stars of different spectral type we use the Rossby number (ratio of the rotational period to the convective turnover time) instead of the rotational period. This ratio is function of stellar mass, and saturation will start to be seen at progressive longer periods for stars with lower masses. *Supersaturated* stars have Rossby Number log N_R<-1.7. In order to compare these sparse, but systematically derived, results with those of other stars, we have computed the temperature-sensitive index, which we define as the ratio of the DEM in the *high* temperature range (logT[K]=6.9-7.6) to the total DEM (logT[K]=6.2-7.6), for a larger sample of rapid rotators culled from analyses in the literature. While a fairly coarse representation of DEM, this temperature index should be quite insensitive to the details of the different methods and data used to derive it.

Table 1: Stellar Parameters and Coronal Abundances[a] Single and Binary Systems

ID	Single Star	SpTy (V)	P_{rot}	log $\Re$	log L_x/L_{bol}	EM_{low}	[Fe/H]	[O/H]	[Si/H]	[Mg/H]	[Ne/Fe]	Ref
1	EK Dra	G0V	2.75	-0.60	-3.53	.627	-0.08	-0.10	-0.09	+0.11	+0.19	[15]
2	47 Cas B	G1V	1.00	-1.05	-4.09	.443	-0.21	-0.09	-0.14	-0.13	+0.43	[15]
3	π^1 Uma	G1V	4.70	-0.23	-4.46	.895	+0.08	-0.22	-0.05	+0.21	-0.20	[15]
4	χ^1 Ori	G1V	5.10	-0.22	-4.55	.962	-0.01	-0.22	-0.10	+0.03	-0.04	[15]
5	κ^1 Cet	G5V	9.20	-0.17	-5.11	.892	+0.12	-0.05	+0.09	+0.34	+0.03	[15]
6	PZ Tel	K0V	0.94	-1.28	-3.11	.349	-0.49	-0.19	-0.55	-0.46	+0.56	[1]
7	AB Dor	K2V	0.51	-1.58	-3.34	.331	-0.52	-0.16	-0.46	-0.51	+0.67	[5]
8	ϵ Eri	K2V	11.03	-0.28	-4.86	.962	-0.08	-0.13	-0.17	-0.10	+0.32	[13]
9	Speedy Mic	K3V	0.38	-1.77	-3.07	.307	-0.75	-0.09	-0.60	-0.70	+1.00	This work
10	Rst 137B	M2V	<0.37	-1.87	-3.00	.534	-0.91	-0.33	-0.63	-0.58	+0.82	This work
11	AD Leo	M3V	2.70	-1.86	-3.34	.649	-0.42	+0.01	-0.13	-0.34	+0.62	[10]
12	EV Lac	M4V	4.38	-1.80	-3.14	.773	-0.52	-0.30	-0.32	-0.61	+0.52	[12]
ID	**Binary Syst.**	**SpTy (V+V)**	**P_{rot}**	**log $\Re$**	**log L_x/L_{bol}**	**EM_{low}**	**[Fe/H]**	**[O/H]**	**[Si/H]**	**[Mg/H]**	**[Ne/Fe]**	**Ref**
13	TZ CrB	F6V/G0V	1.14	-0.60	-3.22	.406	-0.28	-0.17	-0.05	+0.05	+0.34	[11]
14	44 Boo	G0V/G5V	0.28	-1.70	-3.67	.490	-0.78	-0.33	-0.65	-0.67	+0.51	[3]
15	ER Vul	G0V/G5V	0.69	-1.03	-3.10	.418	-0.48	-0.61	-0.49	-0.36	+0.75	[3]
16	SV Cam	G0V/K6V	0.59	-1.34	-3.25	.347	-0.20	+0.27	-0.12	-0.04	+0.64	[14]
17	VW Cep	G5V/K0V	0.25	-1.85	-3.40	.645	-0.67	-0.06	-0.43	-0.33	+0.46	[9]
18	V471 Tau	K2V/WD	0.52	-1.53	-2.79	.477	-0.61	-0.27	-0.46	-0.53	+0.62	[5]
19	YY Gem	M1V/M1V	0.81	-2.16	-3.06	.800	-0.63	-0.26	-0.36	-0.65	+0.71	[6]
ID	**Binary Syst.**	**SpTy (IV+V)**	**P_{rot}**	**log $\Re$**	**log L_x/L_{bol}**	**EM_{low}**	**[Fe/H]**	**[O/H]**	**[Si/H]**	**[Mg/H]**	**[Ne/Fe]**	**Ref**
20	AR Lac	G2IV/K0IV	1.98	-0.90	-3.35	.291	-0.08	+0.05	-0.18	+0.16	+0.52	[8]
21	UX Ari	K0IV/G5V	7.44	-0.53	-3.34	.261	-0.83	-0.30	-0.59	-0.54	+1.33	[3]
22	HR 1099	K1IV/G5V	2.84	-0.87	-3.13	.255	-0.67	-0.04	-0.63	-0.72	+1.05	[4]
23	V851 Cen	K2IV-III/?	12.05	-0.29	-3.52	.378	-0.28	+0.18	-0.58	-0.07	+0.93	[13]
24	II Peg	K2IV-V/?	6.72	-0.54	-2.93	.234	-0.78	+0.26	-0.30	-0.34	+1.36	[7]
25	VY Ari	K3IV-V	13.20	-0.23	···	···	-0.13	-0.69	-0.58	-0.47	+0.96	[2]

[a] Abundances relative to solar photospheric values (Asplund et al. 2005 ASP Conf.Ser. 336).

References: Argiroffi et al. (2004, ApJ, 609, 925); [2] Audard et al. (2004, ApJ, 617, 531); [3] Ball et al. (2007, ApJ, submitted); [4] Drake et al. (2001, ApJ, 548, L81); [5] Garcia-Alvarez et al. (2005, ApJ, 612, 1009); [6] Guedel et al. (2001, A&A, 365, L344); [7] Huenemoerder et al. (2001, ApJ, 559, 1135); [8] Huenemoerder et al. (2003, ApJ, 595, 1131); [9] Huenemoerder et al. (2006, ApJ, 650, 1119); [10] Maggio et al. (2004, ApJ, 613, 548); [11] Osten et al. (2003, ApJ, 582, 1073); [12] Robrade & Schmitt (2005, A&A, 435, 1073); [13] Sanz-Forcada et al. (2004, A&A, 416, 281); [14] Sanz-Forcada et al. (2006, A&A, 445, 673); [15] Telleschi et a. (2005, ApJ, 622, 653).

DEMS AND CORONAL CHEMICAL COMPOSITION

In order to obtain the differential emission measure (DEM) we have performed a Markov-Chain Monte-Carlo analysis using a Metropolis algorithm (MCMC[M]) on the set of supplied line flux ratios (Kashyap & Drake 1998, ApJ, 503, 450). Based on the lines we used in our analysis (O, Ne, Mg, Si, S, FeXVII, FeXVIII and FeXXI) we are able to obtain well-constrained DEMs between logT[K]=6.2 and logT[K]=7.5 (coolest and hottest peak formation temperature in our line set). We can evaluate the abundances, based on the derived DEM, of any elements for which we have lines with measured fluxes.

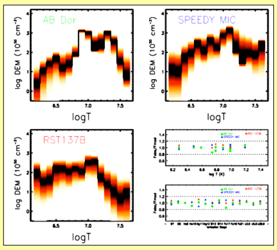

Top and left: DEM obtained by running the MCMC[M] reconstruction code on a set of H-like, He-like and highly ionized Fe line fluxes (O, Ne, Mg, Si, S, Fe17, Fe18, Fe21). The thick solid line represents the best-fit DEM, while the shaded regions correspond to the 1-sigma deviations present in each temperature bin. Bottom right: Comparison of observed and modeled lines fluxes vs ionic species (bottom) and Tmax (top) for the three objects. The 'line-free' continuum spectral regions (1A) are labeled as c followed by the mid-wavelength value.

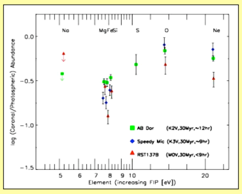

Comparison of coronal abundances vs FIP for the three objects. The abundances were obtained from abundance-independent DEM reconstruction and are relative to the solar photospheric mixture of Asplund et al. (2005, ASPC, 336, 25) with Ne from Drake & Testa (2005, Nature, 436, 525). The error bars represent statistical uncertainties only; true uncertainties are likely to be 0.1dex.

CORONAE OF FAST ROTATORS (CONTD)

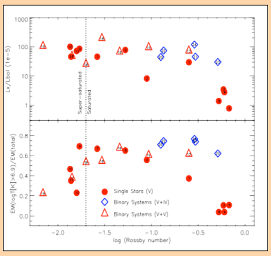

Top left: L_x/L_{bol} vs the Rossby number for the sample of stars in Table 1. This sample includes single dwarfs stars (circles) and binary systems (diamonds and triangles). The labels shown in the symbols are the same as those in Table 1. The demarcation between the saturated and supersaturated regions, based on definition of Randich (1998), is indicated by a dashed vertical line. Bottom left: Same as for top panel but for $\phi_{6.9}$ vs the Rossby number. Top right: O/H and Fe/H coronal abundance vs $\phi_{6.9}$ for the sample of stars in Table 1. The coronal abundance values are expressed relative to the abundance mixture of Asplund et al. (2005) with Ne from Drake & Testa (2005). Middle right: Same as top panels but for the Fe/H coronal abundance vs the Rossby number. Bottom right: Same as top panel but for the Fe/H coronal abundance vs L_x/L_{bol}.

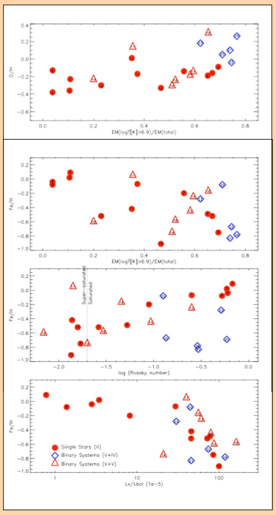

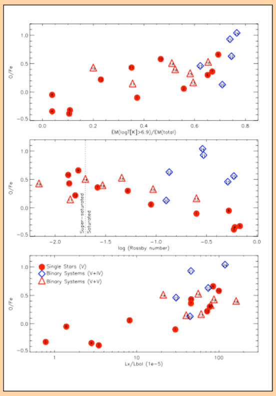

Same as Fig. on the left but for O/Fe.

RESULTS :

(1) The temperature structures of AB Dor, Speedy Mic and Rst 137B all peak at logT[K]~7.0-7.1, though the overall DEM shapes are slightly different. If the DEM trends observed here in only three stars can be generalised, they hint that as supersaturation is reached the DEM slope below the temperature of peak DEM becomes shallower, while the DEM drop-off above this temperature becomes more pronounced.

(2) All three of the stars studied in detail here show evidence for an inverse of the solar-like FIP effect, with smaller coronal abundances of the low FIP elements Mg, Si and Fe, relative to the high FIP elements S, O and Ne. This is consistent with existing coronal abundance studies of other active stars.

(3) In the context of the larger stellar sample, we observe that in dwarf single and binary stars coronal thermal structure shows an increase in the emission of plasma at high temperatures (logT[K]>6.9) as the Rossby number decreases and approaches the saturated-supersaturated boundary. However, once the supersaturated region is reached this trend inverts; supersaturated stars maintain a smaller fraction of coronal plasma at and above 10 million degrees than stars of higher Rossby number. This result is consistent with the tentative generalised DEM behaviour outlined in (1).

(4) The stellar sample shows that coronal Fe abundance is inversely correlated with L_x/L_{bol}, and for dwarfs is also well-correlated with Rossby number. The Fe abundance is seen to decline slowly with rising L_x/L_{bol}, but declines sharply at L_x/L_{bol} >3x10^{-4}.

(5) The are no obvious trends of O abundance with activity indicators. Derived coronal O abundances are perhaps very weakly correlated with the coronal temperature index, with hotter coronae possibly exhibiting larger O abundances. RS CVn-type binaries exhibit systematically larger O abundances than dwarfs; this could be partially due to galactic evolutionary differences in [O/Fe] between dwarf and RS CVn samples.

(6) Coronal O abundances average at values of [O/H]~-0.2. Comparison of coronal and photospheric values for some of the sample suggests that active stellar coronae are in general slightly depleted in O relative to their photospheres.

(7) The coronal O/Fe ratio for dwarfs shows a strong trend of increasing O/Fe with decreasing Rossby number, and appears to saturate at the supersaturation boundary with a value of [O/Fe]~0.5. Similar correlations are seen with O/Fe increasing as a function of coronal temperature index, as revealed in earlier work, and with increasing L_x/L_{bol}. The range in O/Fe variations attributable to differences in coronal properties among the sample is about a factor of 10.